ChemPubSoc Europe

DOI: 10.1002/ejic.201800112

European Journal of Inorganic Chemistry

Full Paper

Polyphosphorus Hybrid Polymers

Organometallic–Organic Hybrid Polymers Assembled from Pentaphosphaferrocene, Bipyridyl Linkers, and Cu^{I} Ions

Mehdi Elsayed Moussa,[a] Stefan Welsch,[a] Matthias Lochner,[a] Eugenia V. Peresypkina,[b,c] Alexander V. Virovets,[b,c] and Manfred Scheer*[a]

Dedicated to Professor Dietmar Stalke on the occasion of his 60th birthday

Abstract: A multicomponent approach of the P_n ligand complex [Cp*Fe(η^5-P_5)] (**1**: Cp* = η^5-C_5Me_5) with the ditopic organic linkers 4,4′-bipyridine (**2**) or *trans*-1,2-di(pyridine-4-yl)ethene (**3**) in the presence of Cu^{I} salts of the anions $[BF_4]^-$ and $[PF_6]^-$ or the coordinating anion Br^-, leads to the formation of four novel organometallic–organic hybrid polymers: the cationic 1D polymeric compounds $[Cu_4\{Cp^*Fe(\mu_3,\eta^{5:1:1}\text{-}P_5)\}_2(\mu,\eta^{1:1}\text{-}C_{10}H_8N_2)_4(CH_3CN)_4]_n[BF_4]_{4n}$ (**4**) and $[Cu_4\{Cp^*Fe(\mu_3,\eta^{5:1:1}\text{-}P_5)\}_2(\mu,\eta^{1:1}\text{-}C_{10}H_8N_2)_4(CH_3CN)_4]_n[PF_6]_{4n}$ (**5**) as well as the unique neutral threefold 2D → 2D interpenetrated networks $[Cu_2Cl_2\{Cp^*Fe(\mu_3,\eta^{5:1:1}\text{-}P_5)\}(\mu,\eta^{1:1}\text{-}C_{12}H_{10}N_2)]_n$ (**6**) and $[Cu_2Br_2\{Cp^*Fe(\mu_3,\eta^{5:1:1}\text{-}P_5)\}(\mu,\eta^{1:1}\text{-}C_{10}H_8N_2)]_n$ (**7**).

Introduction

The design and synthesis of coordination polymers (CPs) have been attracting unprecedented attention in recent years because of their high structural diversity and potential applications in many fields of material science.[1] To date, the most common strategy to synthesize CPs is an one-step reaction of multitopic organic ligands (bearing usually nitrogen-, oxygen-, or sulfur-donor atoms) with transition metal ions.[2] However, several other alternative methods have also been reported, mainly to overcome the difficulties in the control and modification of the targeted assemblies.[3] One of these approaches refers to the use of mixed ligands (mixed-ligand strategy) providing CPs with more structural diversity and remarkable physical properties in comparison to using only one type of ligand.[4] Our group contributed to this field by using polyphosphorus and polyarsenic ligand complexes with flexible coordination modes as organometallic connecters between metal ions. That novel research area allowed the synthesis of 1D, 2D, and 3D CPs,[5] nano-sized fullerene-like supramolecular spherical aggregates[6] and large molecular organometallic capsules.[7] More recently, we started to investigate mixed-ligand reactions of the tetrahedrane complex $[Cp_2Mo_2(CO)_4(\eta^2\text{-}P_2)]$ (Cp = η^5-C_5H_5) in combination with Ag^{I} or Cu^{I} salts and bipyridyl linkers. These reactions allowed the access to unprecedented organometallic–organic hybrid CPs in which organometallic nodes are linked to polycationic chains via organic linkers.[8b–8g] Most recently, we also reported the first series of neutral 2D CPs based on pentaphosphaferrocene (**1**), CuCl and ditopic pyridine-based linkers.[8a] Based on these results, the question arises as to whether it is possible to further enrich this library of hybrid CPs with new neutral and cationic compounds with unprecedented topologies. Herein, we report the reaction of pentaphosphaferrocene (**1**) with Cu^{I} salts of the anions $[BF_4]^-$ and $[PF_6]^-$ or the coordinating anion Br^- in the presence of the ditopic organic linkers 4,4′-bipyridine (**2**) or *trans*-1,2-di(pyridine-4-yl)ethene (**3**). This reaction leads to the formation of four organometallic–organic hybrid CPs: the novel 1D cationic polymeric compounds $[Cu_4\{Cp^*Fe(\mu_3,\eta^{5:1:1}\text{-}P_5)\}_2(\mu,\eta^{1:1}\text{-}C_{10}H_8N_2)_4(CH_3CN)_4]_n[BF_4]_{4n}$ (**4**) and $[Cu_4\{Cp^*Fe(\mu_3,\eta^{5:1:1}\text{-}P_5)\}_2(\mu,\eta^{1:1}\text{-}C_{10}H_8N_2)_4(CH_3CN)_4]_n[PF_6]_{4n}$ (**5**) and the unique neutral threefold 2D → 2D parallel interpenetrated networks $[Cu_2Cl_2\{Cp^*Fe(\mu_3,\eta^{5:1:1}\text{-}P_5)\}(\mu,\eta^{1:1}\text{-}C_{12}H_{10}N_2)]_n$ (**6**) and $[Cu_2Br_2\{Cp^*Fe(\mu_3,\eta^{5:1:1}\text{-}P_5)\}(\mu,\eta^{1:1}\text{-}C_{10}H_8N_2)]_n$ (**7**).

Results and Discussion

The reaction of the *cyclo*-P_5 ligand complex **1** with $[Cu(CH_3CN)_4][BF_4]$ or $[Cu(CH_3CN)_4][PF_6]$ and 4,4′-bipyridine (**2**) in a 1:2:2 stoichiometry[9] in a mixture of CH_2Cl_2 and CH_3CN at room temperature followed by a slow diffusion of *n*-pentane leads to the selective formation of crystals of the compounds **4** (green) and **5** (orange) in good yields [**4** (67 %), **5** (70 %)] suitable for X-ray diffraction studies (Scheme 1). The single-crystal X-ray structure analyses of **4** and **5** (Figure 1), respectively,

[a] *Institut für Anorganische Chemie der Universität Regensburg, 93040 Regensburg, Germany*
E-mail: manfred.scheer@chemie.uni-regensburg.de
http://www.uni-regensburg.de/chemie-pharmazie/anorganische-chemie-scheer/
[b] *Nikolaev Institute of Inorganic Chemistry, Siberian Division of RAS, Lavrentyev prosp. 3, 630090 Novosibirsk, Russia*
[c] *Novosibirsk State University, ul. Pirogova, 2, 630090 Novosibirsk, Russia*

Supporting information and ORCID(s) from the author(s) for this article are available on the WWW under https://doi.org/10.1002/ejic.201800112.

shows that they represent 1D organometallic–organic hybrid CPs with a similar ladder-like structure. The repeating units of the two polymers **4** and **5** consist of four Cu^{I} cations, which are bridged pairwise by a pentaphosphaferrocene unit **1** possessing a 1,2-coordination mode. Together with two linkers **2**, two of the homobimetallic building blocks $[Cu_2(\mathbf{1})(CH_3CN)_2]$ form metallaparacyclophane-like arrays. These arrays are connected via two more linkers **2** to build up the 1D CPs **4** and **5**. As a consequence, the polymers **4** and **5** provide different types of meshes in the 1D polymeric arrangements (Figure 1 and S1), small (rectangular) and large (square) ones with cavities of maximum dimensions of about 1.43 and 1.50 nm, respectively.[10] In the crystal packing of **4** and **5**, the counteranions are located between the chains. However, in each case, two dichloromethane molecules partially occupy each of the large cavities of the meshes. These guest molecules are stabilized by the Cl···π interactions between the chlorine atoms of the CH_2Cl_2 molecules and the π clouds of the pyridyl moieties of the linker **2** [Cl···π(pyridyl centroid) shortest distances: 3.76(5) Å (**4**) and 3.79(2) Å (**5**)]. The organic linkers **2** in the polymers **4** and **5** are well separated from each other (ca. 4.2 Å shortest distance) and therefore do not show any intramolecular π–π stacking interactions. Instead, the first example of P_5···P_5 stacking is observed in the polymers **4** and **5** between the chains with the interplanar P_5···P_5 distances [3.52–3.53 Å (**4**) and 3.57 Å (**5**)], i.e. about 0.2 Å less than the sum of van der Waals radii (Figure S2, see Supporting Information). Similar interactions were only found in spherical supramolecules[11] as host–guest interactions between parallel *cyclo*-P_5 units of the guest molecule **1** and the inner surface of the supramolecule. The P_5···P_5 stacking was, however, featured by longer interplanar distances (3.86–4.03 Å) and was therefore treated as being enforced by encapsulation. In addition, in **4** and **5**, the stacking is *slipped* compared to a *face-to-face* one in the supramolecules. The P–P bond lengths

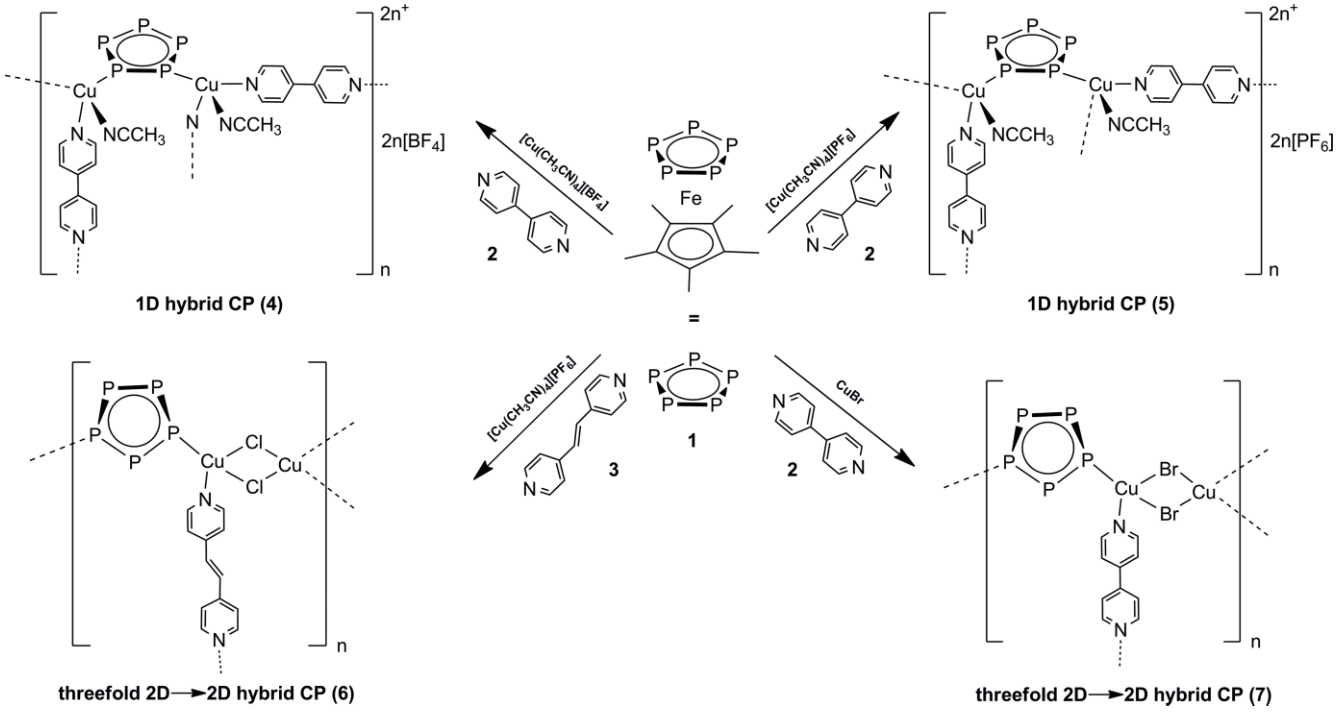

Scheme 1. Overview of the reaction of the *cyclo*-P_5 ligand complex **1** with 2,2′-bipyridine (**2**), *trans*-1,2-di(pyridine-4-yl)ethene (**3**) and Cu^{I} salts.

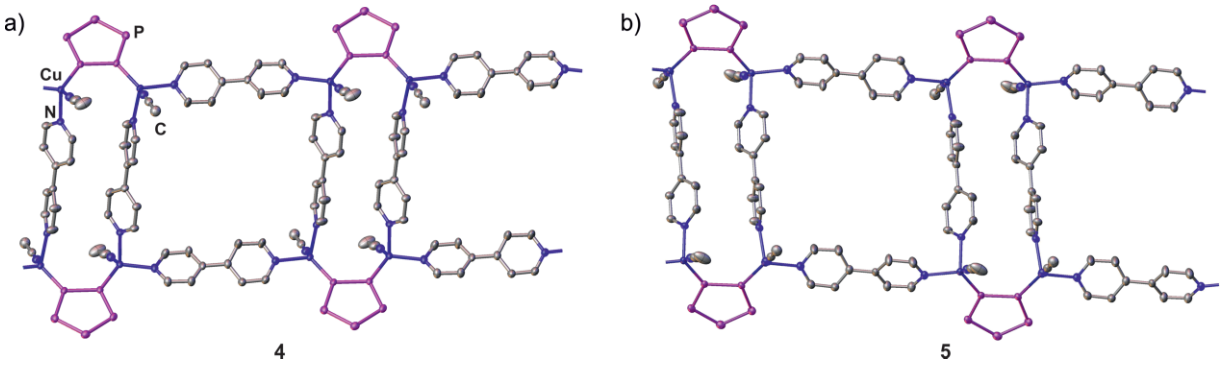

Figure 1. Section of the 1D cationic polymeric networks (a) **4** and (b) **5**, in the solid state. [Cp*FeP_5] are shown as *cyclo*-P_5 moieties; H atoms, counterions as well as solvent molecules are omitted for clarity.

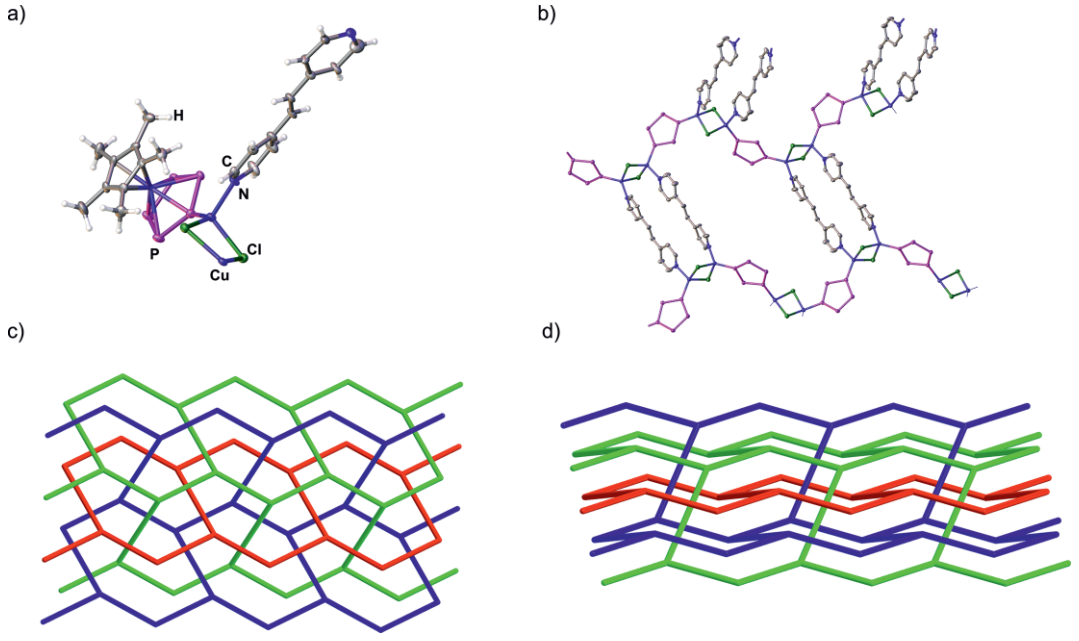

Figure 2. (a) The repeating unit of **6**. (b) Fragment of a single staggered **hcb** layer in the 2D neutral polymeric network **6**; [Cp*FeP$_5$] are shown as *cyclo*-P$_5$ fragments; H atoms are omitted for clarity. (c) Top and d) side simplified views of three interpenetrated layers in **6**.[16]

in **4** [2.106(1)–2.120(3) Å] and **5** [2.103(5)–2.118(2) Å] are comparable to those of the non-coordinated ligand complex **1** (2.117 Å).[12] The Cu–P bond lengths in **4** and **5** are in the range of 2.178(2)–2.194(3) Å. Compounds **4** and **5** are only slightly soluble in donor solvents such as CH_3CN but completely insoluble in other common organic solvents such as CH_2Cl_2, THF and *n*-pentane. Their room temperature $^{31}P\{^1H\}$ NMR spectra in CD_3CN exhibit single signals of –150.5 and –148.2 ppm, which are upfield shifted compared to that of the free ligand complex **1** (δ =152.2 ppm)[5d] revealing no complete degradation of the polymeric structures in solution. Their room temperature ^1H and $^{13}C\{H\}$ NMR spectra in CD_3CN show typical signals for the Cp* ligand and for the linker **2**. In the ESI mass spectra of **4** and **5**, a peak of the cationic fragment [Cu(**1**)(**2**)]$^+$ was detected indicating no full degradation of the polymeric structures in solution (further details see SI).

Upon choosing the slightly longer ligand (**3**) in the reaction between the *cyclo*-P$_5$ ligand complex **1** with [Cu(CH_3CN)$_4$][PF_6] in a mixture of CH_2Cl_2 and CH_3CN, a new compound **6** was formed [Figures 2a and b, and Figures S4,S6 (see SI)] as brown crystals in rather low yield (7 %).[13] Its crystal structure reveals an unprecedented 2D organometallic–organic hybrid polymer with a layered structure of the general formula $[Cu_2Cl_2\{Cp^*Fe(\mu_3,\eta^{5:1:1}\text{-}P_5)\}(\mu,\eta^{1:1}\text{-}C_{12}H_{10}N_2)]_n$ (Figure 2c, d). Obviously, a chlorine abstraction from the solvent CH_2Cl_2 must have taken part, as CuCl was not provided for this reaction. The photocatalytic and thermolytic decomposition of CH_2Cl_2 leading to halogen-containing copper-[14a,14b] and silver-[14c] based polymers was already discovered in the literature.[14] Each 2D layer in **6** is composed as an arrangement of parallel *zig-zag* $[(Cu_2Cl_2)(\mathbf{1})]_n$ 1D chains in which each Cu^I is linked by an additional organic spacer **3** into staggered layers. As a consequence, the network **6** provides different types of meshes in the 2D polymeric layers (Figure 2b), small and large (rectangular) ones with cavities of maximum dimensions of about 1.40 and 2.38 nm, respectively.[10] In the large meshes, the organic linkers **3** are well separated from each other (ca. 11.2 Å shortest distance). In the small meshes, the shortest distance is only about 3.9 Å revealing a possible weak π–π interaction. If these small meshes are not taken into account, the arrangement of the large ones gives a honeycomb net (**hcb**).[15] The large cavities and the staggered geometry of the **hcb** layer give rise to a polycatenation of three similar honeycomb layers, with two parallel layers being inserted into each larger mesh of the third one (Figure 2c, d).[15,16]

The chloride abstraction observed in the latter reaction leading to the unprecedented threefold 2D → 2D parallel polycatenated net motivated us to investigate the possibility to synthesize such neutral networks starting directly from Cu^I halides instead of [Cu(CH_3CN)$_4$][BF_4] or [Cu(CH_3CN)$_4$][PF_6]. The reaction of the *cyclo*-P$_5$ ligand complex **1** with CuBr and 4,4′-bipyridine (**2**) in a 1:2:2 stoichiometry[9] leads to the formation of a new compound **7** as brown crystals in low yields (9 %, Scheme 1).[17] The X-ray structure analysis performed on a single crystal of **7** shows that this compound is a unique neutral 2D polymer of the formula $[Cu_2Br_2\{Cp^*Fe(\mu_3,\eta^{5:1:1}\text{-}P_5)\}(\mu,\eta^{1:1}\text{-}C_{10}H_8N_2)]_n$ (Figures S5, S7 see SI). The derivative **7** is isotypic to the network **6** with $[(Cu_2Br_2)(\mathbf{1})]_n$ instead of $[(Cu_2Cl_2)(\mathbf{1})]_n$ 1D chains in **6** and of the same topological type. Each Cu^I in **7** is linked by an additional organic spacer **2** instead of the linker **3** in **6**. Similarly to **6**, the polymer **7** shows two types of rectangular meshes, small and large ones with relatively smaller cavities (maximum dimensions of ca. 1.17 and 2.03 nm, respectively).[10] The organic linkers **2** within the small meshes are also located close to each other with the shortest interplanar distance of about 3.3 Å, which is reminiscent of π–π interaction. Despite the smaller mesh size in **7** compared with **6**, the same type of threefold parallel polycatenation is realized (Figure S7). The P–P bond

lengths in **6** [2.111(6)–2.120(5) Å] and **7** [2.106(7)–2.114(4) Å] are comparable to those of the polymers **4** and **5** and of the non-coordinated ligand complex **1** (2.117 Å).[12] The Cu–P bond lengths in **6** and **7** are in the range between 2.204(9) and 2.205(9) Å, a little elongated as compared to those in the polymers **4** and **5**. This slight elongation is most probably due to the different coordination modes of the *cyclo*-P_5 ligand of **1** in the two types of polymers: the 1,2-mode in the 1D polymers **4** and **5** and the 1,3-mode in the 2D polymers **6** and **7**.

The derivatives **6** and **7** are insoluble in common organic solvents and also in donor solvents such as CH_3CN. Therefore, these unique compounds were only structurally characterized by X-ray single crystal structure analysis.

Conclusions

The obtained results show the possibility to use the pentaphosphaferrocene complex **1** in a mixed ligand approach with the organic bipyridyl linkers 4,4′-bipyridine (**2**) or *trans*-1,2-di(pyridine-4-yl)ethene (**3**) and a number of Cu^I salts to synthesize a new series of cationic and neutral organometallic–organic hybrid CPs. Notably, the flexible coordination mode of the pentaphosphaferrocene **1** allows the synthesis of CPs with different dimensionalities: In the 1D CPs **4** and **5**, the *cyclo*-P_5 ligand of **1** is connected in a 1,2-mode, whereas the 2D networks **6** and **7** show a 1,3-coordination mode. Interestingly, in the crystal structures of **4** and **5**, unique P_5···P_5 stacking interactions are found featured by very short interplane distances of 3.52–3.79 Å. In the networks **6** and **7**, the P_5···P_5 stacking interactions are not realized, however, a unique threefold parallel polycatenation of the honeycomb layers is observed. In the crystal structures of all CPs **4**–**7**, two types of meshes are observed with maximum dimensions ranging between about 1.17 and 2.38 nm. Current studies involve the use of pentaphosphaferrocene with multitopic pyridine-based linkers and CuX (X = Cl, Br, I) for a possible access to a new class of neutral 3D organometallic–organic hybrid networks.

Experimental Section

General Considerations: All experiments were performed under an atmosphere of dry argon using standard Schlenk techniques. 4,4′-bipyridine (**2**), trans-1,2-di(pyridine-4-yl)ethene (**3**) and the copper salts: $[Cu(CH_3CN)_4][BF_4]$, $[Cu(CH_3CN)_4][PF_6]$, CuCl and CuBr were purchased from Alfa Aesar and used as received without further purification. The P_n ligand complex $[Cp^*Fe(\eta^5\text{-}P_5)]$ (**1**)[18] was synthesized according to literature procedure. Solvents were freshly distilled under argon from CaH_2 (CH_2Cl_2, CH_3CN) and from Na/K alloy (*n*-pentane). The ^1H, ^{13}C, ^{31}P and ^{19}F NMR spectra were recorded on a Bruker Avance 400 spectrometer. ^1H and ^{13}C NMR chemical shifts were reported in parts per million (ppm) relative to Me_4Si as external standard. ^{31}P NMR chemical shifts were expressed in ppm relative to external 85 % H_3PO_4 and were decoupled from the protons. ^{19}F NMR chemical shifts were reported relative to $CFCl_3$. For the ESI-MS a Finnigan Thermoquest TSQ 7000 mass spectrometer was used. Elemental analyses were performed by the microanalytical laboratory of the University of Regensburg.

Synthesis of 4: A solution of $[Cu(CH_3CN)_4][BF_4]$ (47 mg, 0.15 mmol) and $[Cp^*Fe(\eta^5\text{-}P_5)]$ (**1**; 26 mg, 0.075 mmol) in a mixture of CH_2Cl_2 (10 mL) and CH_3CN (10 mL) was stirred for 10 min at ambient temperature. Afterwards a solution of 4,4′-bipyridine (**2**; 24 mg, 0.15 mmol) in CH_2Cl_2 (2 mL) was added. The mixture was stirred for 3 h at room temperature and filtered. Crystals of compound **4**·$5CH_2Cl_2$ suitable for single-crystal X-ray structure analysis were grown through slow diffusion of *n*-pentane to this solution. The formed crystals were filtered off, washed with *n*-pentane (3 × 2 mL) and dried in vacuo. According to the elemental analysis approximately two CH_2Cl_2 molecules per formula unit remained. Yield: 57 mg (67 %). ^1H NMR (CD_3CN, 400 MHz): δ = 1.42 [s; $C_5(CH_3)_5$], 1.95 (s; CH_3CN), 7.68 (m, H_{pyr}), 8.69 (m, H_{pyr}) ppm. $^{13}C\{^1H\}$ NMR (CD_3CN, 101 MHz): δ = 11.0 [s; $C_5(CH_3)_5$], 92.6 [$C_5(CH_3)_5$], 122.5 (s; C_{pyr}), 146.2 (s; C_{pyr}), 151.6 (s; C_{pyr}) ppm. $^{31}P\{^1H\}$ NMR (CD_3CN, 162 MHz): δ = –150.5 (s) ppm. $^{19}F\{^1H\}$ NMR (CD_3CN, 282 MHz): δ = –150.6 (s) ppm. Positive ion ESI-MS (CH_3CN): *m/z* (%) = 755.0 (16) $[Cu(Cp^*FeP_5)_2]^+$, 565.1 (13) $[Cu(Cp^*FeP_5)(C_{10}H_8N_2)]^+$, 450.0 (100) $[Cu(Cp^*FeP_5)(CH_3CN)]^+$. $C_{68}H_{74}B_4Cu_4F_{16}Fe_2N_{12}P_{10}$·$2CH_2Cl_2$ (2252.12 g mol^{-1}): calcd. C 37.33, H 3.49, N 7.46; found C 37.92, H 3.67, N 6.94.

Synthesis of 5: A solution of $[Cu(CH_3CN)_4][PF_6]$ (56 mg, 0.15 mmol) and $[Cp^*Fe(\eta^5\text{-}P_5)]$ (**1**; 26 mg, 0.075 mmol) in a mixture of CH_2Cl_2 (10 mL) and CH_3CN (10 mL) was stirred for 10 min at ambient temperature. Afterwards a solution of 4,4′-bipyridine (**2**; 24 mg, 0.15 mmol) in CH_2Cl_2 (2 mL) was added. The mixture was stirred for 3 h at room temperature and filtered. Crystals of compound **5**·$0.6CH_2Cl_2$·$0.5CH_3CN$ suitable for single-crystal X-ray structure analysis were grown through slow diffusion of *n*-pentane to this solution. The formed crystals were filtered off, washed with *n*-pentane (3 × 2 mL) and dried in vacuo. Yield: 60 mg (70 %). ^1H NMR (CD_3CN, 300 MHz): δ = 1.44 [s; $C_5(CH_3)_5$], 1.94 (s; CH_3CN), 7.62–7.71 (m, H_{pyr}), 8.63 ppm (m, H_{pyr}); $^{13}C\{^1H\}$ NMR (CD_3CN, 75.47 MHz): δ = 16.0 [s; $C_5(CH_3)_5$], 92.8 [$C_5(CH_3)_5$], 120.4 (s; C_{pyr}), 148.0 (s; C_{pyr}), 152.1 ppm (s; C_{pyr}); $^{31}P\{^1H\}$ NMR (CD_3CN, 121.49 MHz): δ = –148.2 (s), –144.2 ppm (m, PF_6^-); $^{19}F\{^1H\}$ NMR (CD_3CN, 282.40 MHz): δ = –72.3 ppm (d, PF_6^-); positive ion ESI-MS (CH_3CN): *m/z* (%) = 755.5 (33) $[Cu(Cp^*FeP_5)_2]^+$, 565.7 (28) $[Cu(Cp^*FeP_5)(C_{10}H_8N_2)]^+$, 450.0 (94) $[Cu(Cp^*FeP_5)(CH_3CN)]^+$. $C_{34}H_{37}Cu_2F_{12}FeN_6P_7$ (1157.43 g mol^{-1}): calcd. C 35.28, H 3.22, N 7.26; found C 35.77, H 3.31, N 7.35.

Synthesis of 6: A solution of $[Cu(CH_3CN)_4][PF_6]$ (56 mg, 0.15 mmol) and $[Cp^*Fe(\eta^5\text{-}P_5)]$ (**1**; 26 mg, 0.075 mmol) in a mixture of CH_2Cl_2 (10 mL) and CH_3CN (10 mL) was stirred for 10 min at ambient temperature. Afterwards a solution of 1,2-di(4-pyridyl)ethylene (**3**; 28 mg, 0.15 mmol) in CH_2Cl_2 (2 mL) was added. The mixture was stirred for 3 h at room temperature and filtered. Crystals of compound **6** suitable for single-crystal X-ray structure analysis were grown within few weeks through slow diffusion of *n*-pentane to this solution. The formed crystals were filtered off, washed with *n*-pentane (3 × 2 mL) and dried in vacuo. Yield: 4 mg (7 %).

Synthesis of 7: A solution of CuBr (22 mg, 0.15 mmol) and $[Cp^*Fe(\eta^5\text{-}P_5)]$ (**1**; 26 mg, 0.075 mmol) in a mixture of CH_2Cl_2 (10 mL) and CH_3CN (10 mL) was stirred for 10 min at ambient temperature. Afterwards a solution of 4,4′-bipyridine (**2**; 24 mg, 0.15 mmol) in CH_2Cl_2 (2 mL) was added. The mixture was stirred for 3 h at room temperature and filtered. Crystals of compound **7** suitable for single-crystal X-ray structure analysis were grown through slow diffusion of *n*-pentane to this solution. The formed crystals were filtered off, washed with *n*-pentane (3 × 2 mL) and dried in vacuo. Yield: 5 mg (9 %).

X-ray Crystallography

Single crystals suitable for single-crystal X-ray structure analysis were obtained for derivatives **4**, **5**, **6**, and **7** as reported above.

The reflection intensities were collected either on an Gemini R-Ultra (Agilent Technologies) equipped with a Ruby (**4**) or an Atlas (**5**) detector, or Rigaku Oxford Diffraction SuperNova diffractometer (former Agilent Technologies) equipped with a Titan (**6**, **7**) detector with Cu$K\alpha$ radiation (λ = 1.54178 Å) using 0.5° or 1° ω scans. The data processing was performed with *CrysAlisPro*.[19] Absorption corrections were applied analytically based on crystal faces.[20] The structures were solved by SheIXT.[21] The *SHELXL-2014/7* program was used to refine the structures by full-matrix least-squares based on F^2. All non-hydrogen atoms were refined with anisotropic displacement parameters. Hydrogen atoms were set in calculated positions and included into refinement with isotropic displacement parameters riding on pivot atoms.

In **4** two of four independent counter anions $[BF_4]^-$ are disordered over two close positions. The ratios of the disordered components were refined with equated isotropic displacement parameters and fixed at resulting values of 0.59/0.41 and 0.52/0.48. The atoms of both disordered components were further refined anisotropically. One of CH_2Cl_2 solvent molecules is also disordered over two positions with a relative weight of the components 0.83/0.17 refined as described.

In **5** solvent molecules of CH_2Cl_2 and MeCN are disordered in the cavities of the polymeric structure. In one position, one MeCN and two CH_2Cl_2 molecules overlap with the molecular occupancy factors refined as 0.50/0.15/0.10. Another two CH_2Cl_2 molecules occupy their close positions with 0.2 and 0.15 occupancies. Larger counter anions $[SbF_6]^-$ are ordered in similar cavities.

In **6** the ligand **3** is disordered over two overlapping positions which mutual contribution was refined as 0.6/0.4. The atoms of both disordered components were refined in anisotropic approximation (Figure S4b).

Further details are given in Table S1. Drawings of the crystal structures (Figures S1–S5) were prepared with *Olex2*.[22] Tables S2–S4 include detailed information on relevant bond lengths and angles.

The analysis of intermolecular interactions and topological features of the crystal structures **4**, **5**, **6** and **7** (Figures S6–S7) was performed using *TOPOSPro*.[16]

CCDC 1816116 (for **4**), 1816117 (for **5**), 1816118 (for **6**), and 1816119 (for **7**) contain the supplementary crystallographic data for this paper. These data can be obtained free of charge from The Cambridge Crystallographic Data Centre.

Acknowledgments

The European Research Council (ERC) is acknowledged for the support in the SELFPHOS ERC-2013-AdG-339072 project.

Keywords: Ferrocene ligands · Hybrid polymers · Coordination modes · Copper · Ligand effects

[1] a) A. Winter, U. S. Schubert, *Chem. Soc. Rev.* **2016**, *45*, 5311–5357; b) X. Zhang, W. Wang, Z. Hu, G. Wang, K. Uvdal, *Coord. Chem. Rev.* **2015**, *284*, 206–235; c) C. He, D. Liu, W. Lin, *Chem. Rev.* **2015**, *115*, 11079–11108; d) T. R. Cook, Y.-R. Zheng, P. J. Stang, *Chem. Rev.* **2013**, *113*, 734–777; e) W. L. Leong, J. J. Vittal, *Chem. Rev.* **2011**, *111*, 688–764.

[2] a) E. Lee, H. Ju, S. Kim, K.-M. Park, S. S. Lee, *Cryst. Growth Des.* **2015**, *15*, 5427–5436; b) E. Lee, K.-M. P, M. Ikeda, S. Kuwahara, Y. Habata, S. S. Lee, *Inorg. Chem.* **2015**, *54*, 5372–5383; c) R. Chakrabarty, P. S. Mukherjee, P. J. Stang, *Chem. Rev.* **2011**, *111*, 6810–6918; d) F. A. Cotton, E. V. Dikarev, M. A. Petrukhina, *Angew. Chem. Int. Ed.* **2001**, *40*, 1521–1523; *Angew. Chem.* **2001**, *113*, 1569.

[3] a) G. Dura, M. C. Carrion, F. A. Jalon, B. R. Manzano, A. M. Rodriguez, K. Mereiter, *Cryst. Growth Des.* **2015**, *15*, 3321–3331; b) G. Kumar, R. Gupta, *Chem. Soc. Rev.* **2013**, *42*, 9403–9453; c) B. Nohra, Y. Yao, C. Lescop, R. Reau, *Angew. Chem. Int. Ed.* **2007**, *46*, 8242–8245; *Angew. Chem.* **2007**, *119*, 8390; d) Z. Qin, M. C. Jennings, R. J. Puddephatt, *Chem. Eur. J.* **2002**, *8*, 735–738; e) M. J. Irwin, J. J. Vittal, G. P. Yap, R. J. Puddephatt, *J. Am. Chem. Soc.* **1996**, *118*, 13101–13102; f) F. A. Cotton, C. Lin, C. A. Murillo, *Proc. Natl. Acad. Sci. USA* **2002**, *99*, 4810–4813; g) F. A. Cotton, C. Lin, C. A. Murillo, *Acc. Chem. Res.* **2001**, *34*, 759–771.

[4] a) J.-Z. Gu, Y.-H. Cui, J. Wu, A. M. Kirillov, *RSC Adv.* **2015**, *5*, 78889–78901; b) J.-M. Hao, B.-y. Yu, K. V. Hecke, G.-H. Cui, *CrystEngComm* **2015**, *17*, 2279–2293; c) Y.-Y. Yang, Z.-J. Lin, T.-T. Liu, T.-T. Liu, J. Liang, R. Cao, *CrystEngComm* **2015**, *17*, 1381–1388; d) D. Sun, Z.-H. Yan, V. A. Blatov, L. Wang, D.-F. Sun, *Cryst. Growth Des.* **2013**, *13*, 1277–1289; e) X.-T. Zhang, L.-M. Fan, X. Zhao, D. Sun, D.-C. Li, J.-M. Dou, *CrystEngComm* **2012**, *14*, 2053–2061.

[5] a) M. E. Moussa, M. Fleishmann, E. V. Peresypkina, L. Dütsch, M. Seidl, G. Balázs, M. Scheer, *Eur. J. Inorg. Chem.* **2017**, *2017*, 3222–3226; b) C. Heindl, A. Kuntz, E. V. Peresypkina, A. V. Virovets, M. Zabel, D. Lüdeker, G. Brunklaus, M. Scheer, *Dalton Trans.* **2015**, *44*, 6502–6509; c) C. Heindl, E. V. Peresypkina, A. V. Virovets, V. Y. Komarov, M. Scheer, *Dalton Trans.* **2015**, *44*, 10245–10252; d) M. Fleischmann, S. Welsch, E. V. Peresypkina, A. V. Virovets, M. Scheer, *Chem. Eur. J.* **2015**, *21*, 14332–14336; e) F. Dielmann, C. Heindl, F. Hastreiter, E. V. Peresypkina, A. V. Virovets, R. M. Gschwind, M. Scheer, *Angew. Chem. Int. Ed.* **2014**, *53*, 13605–13608; *Angew. Chem.* **2014**, *126*, 13823; f) E.-M. Rummel, M. Eckhardt, M. Bodensteiner, E. V. Peresypkina, W. Kremer, C. Gröger, M. Scheer, *Eur. J. Inorg. Chem.* **2014**, *2014*, 1625–1637; g) H. Krauss, G. Balázs, M. Bodensteiner, M. Scheer, *Chem. Sci.* **2010**, *1*, 337–342; h) M. Scheer, L. J. Gregoriades, A. V. Virovets, W. Kunz, R. Neueder, I. Krossing, *Angew. Chem. Int. Ed.* **2006**, *45*, 5689–5693; *Angew. Chem.* **2006**, *118*, 5818; i) J. Bai, A. V. Virovets, M. Scheer, *Angew. Chem. Int. Ed.* **2002**, *41*, 1737–1740; *Angew. Chem.* **2002**, *114*, 1808.

[6] a) E. V. Peresypkina, C. Heindl, A. V. Virovets, M. Scheer, *Struct. Bonding* **2016**, *174*, 321–373; b) C. Heindl, E. V. Peresypkina, D. Lüdeker, G. Brunklaus, A. V. Virovets, M. Scheer, *Chem. Eur. J.* **2016**, *22*, 2599–2604; c) C. Heindl, E. V. Peresypkina, A. V. Virovets, W. Kremer, M. Scheer, *J. Am. Chem. Soc.* **2015**, *137*, 10938–10941; d) M. Fleischmann, S. Welsch, H. Krauss, M. Schmidt, M. Bodensteiner, E. V. Peresypkina, M. Sierka, C. Gröger, M. Scheer, *Chem. Eur. J.* **2014**, *20*, 3759–3768; e) see ref.[5e] f) M. Scheer, A. Schindler, R. Merkle, B. P. Johnson, M. Linseis, R. Winter, C. E. Anson, A. V. Virovets, *J. Am. Chem. Soc.* **2007**, *129*, 13386–13387; g) J. Bai, A. V. Virovets, M. Scheer, *Science* **2003**, *300*, 781–783; h) C. Heindl, E. Peresypkina, A. V. Virovets, I. S. Bushmarinov, M. G. Medvedev, B. Krämer, B. Dittrich, M. Scheer, *Angew. Chem. Int. Ed.* **2017**, *56*, 13237–13243; *Angew. Chem.* **2017**, *129*, 13420.

[7] S. Welsch, C. Groeger, M. Sierka, M. Scheer, *Angew. Chem. Int. Ed.* **2011**, *50*, 1435–1438; *Angew. Chem.* **2011**, *123*, 1471.

[8] a) M. E. Moussa, B. Attenberger, E. V. Peresypkina, M. Scheer, *Dalton Trans.* **2018**, *47*, 1014–1017; b) M. E. Moussa, B. Attenberger, M. Seidl, A. Schreiner, M. Scheer, *Eur. J. Inorg. Chem.* **2017**, *2017*, 5616–5620; c) M. E. Moussa, M. Seidl, G. Balazs, A. V. Virovets, B. Attenberger, A. Schreiner, M. Scheer, *Chem. Eur. J.* **2017**, *23*, 16199–16203; d) M. E. Moussa, B. Attenberger, M. Fleischmann, A. Schreiner, M. Scheer, *Eur. J. Inorg. Chem.* **2016**, *2016*, 4538–4541; e) M. E. Moussa, B. Attenberger, E. V. Peresypkina, M. Fleischmann, G. Balázs, M. Scheer, *Chem. Commun.* **2016**, *52*, 10004–10007; f) B. Attenberger, E. V. Peresypkina, M. Scheer, *Inorg. Chem.* **2015**, *54*, 7021–7029; g) B. Attenberger, S. Welsch, M. Zabel, E. Peresypkina, M. Scheer, *Angew. Chem. Int. Ed.* **2011**, *50*, 11516–11519; *Angew. Chem.* **2011**, *123*, 11718.

[9] Several stoichiometric ratios of the starting material were tested, however, in each case, the mentioned 1:2:2 stoichiometry gave the product in best yields.

[10] Calculated from the largest distance between the Cu^+ ions minus the doubled ionic radius of Cu^+ for the coordination number 4 (0.74 Å).

[11] M. Scheer, A. Schindler, J. Bai, B. P. Johnson, R. Merkle, R. Winter, A. V. Virovets, E. V. Peresypkina, V. A. Blatov, M. Sierka, H. Eckert, *Chem. Eur. J.* **2010**, *16*, 2092–2107.

[12] R. Blom, T. Brück, O. J. Scherer, *Acta Chem. Scand.* **1989**, *43*, 458–462.

[13] The isolation of **6** in low yield is probably due to the presence of only a little amount of chlorine (under these reaction conditions) to be abstracted from the dichloromethane solvent. Attempts to isolate this compound from a similar reaction using CuCl instead of $[Cu(CH_3CN)_4][PF_6]$ failed. Instead, another 2D polymer was formed, which was recently reported (see ref.[8a]).

[14] a) C. E. Anson, L. Ponikiewski, A. Rothenberger, *Z. Anorg. Allg. Chem.* **2006**, *632*, 2402–2404; b) B.-J. Liaw, T. S. Lobana, Y.-W. Lin, J.-C. Wang, C. W. Liu, *Inorg. Chem.* **2005**, *44*, 9921–9929; c) C. W. Liu, B.-J. Liaw, L.-S. Liou, J.-C. Wang, *Chem. Commun.* **2005**, 1983–1985; d) K. J. Doyle, H. Tran, M. Baldoni-Olivencia, M. Karabulut, P. E. Hoggard, *Inorg. Chem.* **2008**, *47*, 7029–7034; e) E. Sanhueza, J. Heicklen, *J. Phys. Chem.* **1975**, *79*, 7–11.

[15] L. Carlucci, G. Ciani, D. M. Proserpio, T. G. Mitina, V. A. Blatov, *Chem. Rev.* **2014**, *114*, 7557–7580.

[16] V. A. Blatov, A. P. Shevchenko, D. M. Proserpio, *Cryst. Growth Des.* **2014**, *14*, 3576–3586. *ToposPro* is available at http://www.topospro.com.

[17] Several attempts to isolate **7** in a better yield were not successful. Also, the precipitation of analytically pure **7** from the crude reaction mixture failed, which was proven by an elemental analysis performed from the isolated powder.

[18] O. J. Scherer, T. Brück, G. Wolmershäuser, *Chem. Ber.* **1988**, *121*, 935–938.

[19] *CrysAlisPro*, different versions **2006–2017**, Rigaku Oxford Diffraction.

[20] R. C. Clark, J. S. Reid, *Acta Crystallogr., Sect. A* **1995**, *51*, 887–897.

[21] G. M. Sheldrick, *Acta Crystallogr., Sect. A* **2015**, *71*, 3–8.

[22] O. V. Dolomanov, L. J. Bourhis, R. J. Gildea, J. A. K. Howard, H. Puschmann, *J. Appl. Crystallogr.* **2009**, *42*, 339–341.

Received: January 25, 2018